DESIGN OF A DISTRIBUTED STRAIN MONITORING SYSTEM FOR HDPE WATER PIPELINES CROSSING AN EARTHQUAKE FAULT

Peter Hubbard
Department of Civil and Environmental Engineering
University of California
Berkeley, CA, USA

Linqing Luo
Lawrence Berkeley National Laboratory
Berkeley, CA, USA

Andrew Yeskoo
Department of Civil and Environmental Engineering
University of California
Berkeley, CA, USA

Kenichi Soga
Department of Civil and Environmental Engineering
University of California
Berkeley, CA, USA

Krista (Moita) Araica
East Bay Municipal Utility District
Oakland, CA, USA

Gus Cicala
East Bay Municipal Utility District
Oakland, CA, US

Marshall McLeod
East Bay Municipal Utility District
Oakland, CA, US

KEYWORDS

High Density Polyethylene, Fiber Optic Sensing, Distributed Strain Sensing, Earthquake Fault

ABSTRACT

Seismically active faults pose a risk to buried water pipelines that can be complicated to quantify. Fault type, slip rate, pipeline geometry, and soil conditions all factor into a complex soil-pipeline interaction. For critical pipelines that cross faults, high-density polyethylene (HDPE) has become an attractive material choice because of its accommodation of large deformations. Using HDPE increases the robustness of these pipelines, but it does not inform a utility about the actual deformed condition of a pipeline. This may be viewed as simply pushing a large break into the future when fault displacements are sufficient to rupture the pipe. By adding a distributed monitoring system to HDPE pipelines, the solution both increases the robustness of the water system and provides an information source that can be leveraged to make asset management decisions in the future, such as intervening measures to reduce stress buildup in a pipeline that has heavily deformed due to fault slippage. In this work, a distributed monitoring system has been designed to monitor two HDPE water pipelines that cross a strike-slip fault in California, USA. The system is based on fiber *optic distributed strain sensing (DSS). The design process of the monitoring system is presented, as well as laboratory tests and lesson learned.*

NOMENCLATURE

$\varepsilon_{b,\max}$	Maximum bending strain
$\varepsilon_{b,\beta}$	Bending strain at angle β from pipe's neutral axis
x	Location along pipe
ε_a	Axial strain
ε_{NA}	Strain at the neutral access
$\varepsilon_{NA+45°}$	Strain at 45 degree from the neutral access
κ	Pipe curvature
c	Outer radius of pipe
θ	Slope of pipe
L	Length of pipe
dx	Spacing of strain measurements
v_b	Pipe deflection due to bending strain
v_a	Pipe deflection due to axial strain
v_t	Total pipe deflection
C	Constant of integration

INTRODUCTION

Pipeline performance at fault crossings is a major concern for utilities in seismically active regions. Many of the concerns relevant to fault crossings are also applicable for differential movements caused by landslides, soil movements from tunneling or deep excavations, and subsidence from dewatering or mining processes (O'Rourke et al. 2016). Therefore, the monitoring method presented here can be easily modified for other geohazards and is not exclusive to fault crossings. Nonetheless, this study focuses on monitoring two high density polyethylene (HDPE) pipelines for their structural behavior associated with permanent ground deformation (PGD) at a fault crossing. Long-term PGD associated with fault creep and immediate PGD due to fault rupture during an earthquake are expected at the installation site. A suitable monitoring method needs to be (1) highly robust to survive in the subsurface for the design-life of the pipe, (2) sensitive enough to measure strains caused by a slowly creeping fault, (3) able to localize deformation within an uncertain faulting region and (4) provide adequate coupling with the HDPE surface of the monitored pipes.

Distributed fiber optic sensing (DFOS) is a platform of sensing technologies that can provide spatially continuous information about an optical fiber. The optical fiber is used as a sensing element and can be attached to an object to make observations about it over a long distance, without the need for many point sensors. DFOS can be used to measure strain, temperature, or vibration depending on the interrogation method used to examine the sensing fiber (Kechavarzi et al. 2016). An interrogator, sometimes referred to as an analyzer, is the acquisition unit that houses a laser, photodetector, digitizer and other hardware components to make the observations about a sensing fiber. Since the interrogator unit is where all the actual sensing is done, the optical fiber sensing element is totally inert (Soga and Luo 2018). Different types of light backscatter are used in sensing applications. In this study, Brillouin scattering-based distributed temperature and strain sensing (DSTS) is applied. Brillouin backscatter is an ideal tool for examining both long term strain and temperature changes. The frequency of Brillouin backscatter shifts linearly with the temperature and strain of the sensing optical fiber, making absolute and long-term measurements possible.

PLANNED PIPELINE INSTALLATION

The East Bay Municipal Utility District (EBMUD) is planning to replace two steel potable water transmission pipelines which cross the active Hayward fault and have experienced numerous leaks. The pipelines will be replaced with two HDPE pipelines, 22” and 36” in diameter, in the vicinity of the fault crossing. The geometry is shown in Figure 1. The pipelines will cross the right-lateral strike-slip fault at a bend, which introduces uncertainty in the exact angle of incidence. The angle between the pipelines and the fault is estimated to be between 75° and 15°.

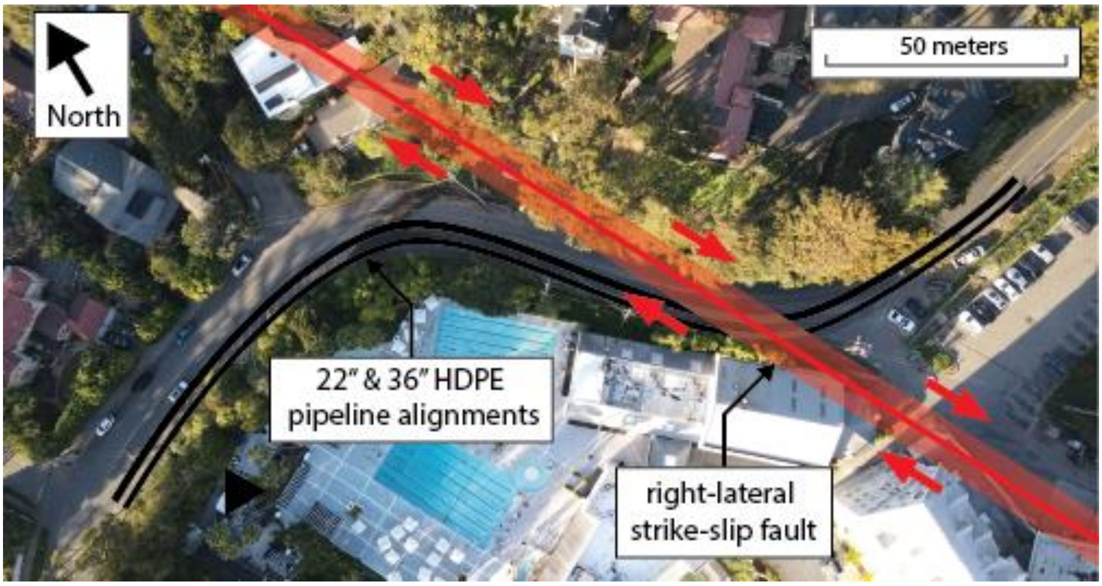

Figure 1. Fault crossing geometry for parallel EBMUD water pipelines

The pipes are expected to experience tensile strain and bending due to fault creep, which is currently estimated as 4 mm per year (Lienkaemper et al. 2012). In addition, the fault may rupture during an earthquake, severely deforming the pipes. Therefore, it is desired to install a monitoring system that can both evaluate the deformed shape of the pipes over time due to the slowly creeping fault movements and assess their integrity after a major acute event. In addition, the exact localization of fault movements is unknown. The behavior of the pipes during fault creep may have strain in a slightly different location than during a fault rupture. For these reasons, distributed fiber optic sensing (DFOS) is an ideal solution. DFOS can both localize deformations and provide a holistic deformation assessment of the pipelines.

DISTRIBUTED STRAIN AND TEMPERATURE SENSING SYSTEM

A distributed strain and temperature sensing system has been designed to meet the specifications of the HDPE pipeline monitoring application. The system can provide strain measurements every 2cm along a 2km-long optical fiber with a spatial resolution of 1m and a strain resolution of 20με.

The system is based on Brillouin optical time-domain reflectometry (BOTDR). BOTDR examines light that is reflected back to the source within an optical fiber at a different frequency than the incident light. Specifically, thermally generated acoustic phonons within the optical fiber matrix cause spontaneous Brillouin scattering at both a decreased (Stokes) and increased (anti-Stokes) frequency. These frequencies shift linearly with respect to the strain and temperature of the fiber at the scattering location. The system employed here (Soga, 2018) uses a heterodyne architecture and the short-time Fourier transform (STFT) to measure the peak Stokes Brillouin frequency within the backscattered light for every 2cm along the fiber (Luo et al. 2019).

After the spectra have been determined for each location on the sensing fiber, the peak Stokes Brillouin frequency is extracted. It is the peak frequency that is then compared from one reading to another to determine the change in temperature or strain that has occurred between readings. The frequency shift is linearly related to the external strain or temperature by a factor that is unique to each sensing cable. A laboratory calibration must be performed to determine the strain and temperature coefficients for a given cable. Furthermore, it is crucial to be able to separate the temperature effect from the strain effect on the Brillouin spectrum. For pipelines, this can be done using parallel sensing fibers with one tightly coupled to the pipeline to ensure strain transfer, while the other is isolated from strain and only records temperature effects.

To sense strain effectively, a coupling method is needed to transfer the mechanical strain from the HDPE pipe surface to the fiber optic core. This can be broken down into two components; effectively transfer strain from (1) the cable sheath to the fiber optic core and (2) from the HDPE pipe to the cable sheath. The first is achieved through cable selection. NanZee Sensing 5mm-diameter sensing cable has been selected for this monitoring application. The cross-section of this cable is shown in Figure 2. The cable consists of a single-mode optical fiber surrounded by a tight buffer. This tight buffer is helically wound within six steel braids. This entire structure is tightly encased within a polyethylene sheath. This cable has been used successfully in many civil engineering applications, such as monitoring strain in concrete piles, retaining walls and compacted soil stratigraphy (Zhang et al. 2019).

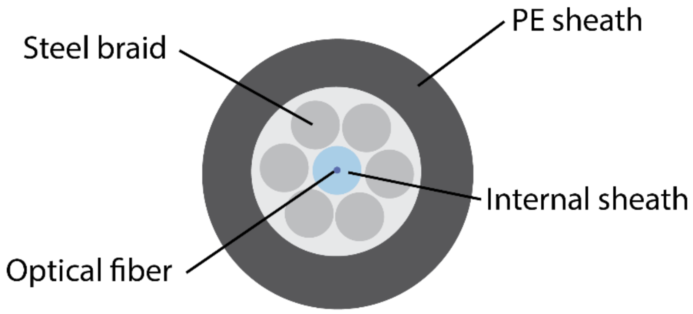

Figure 2. NZS-DSS-C02 cable cross-section

Next, the cable's exterior must be coupled to the pipe surface. A testing campaign at the EBMUD's Oakport facility and UC Berkeley's Richmond field station was conducted to evaluate an effective and practical method of attachment for field installation. In the testing campaign, 20" DR11 HDPE pipes were instrumented with the DSTS system using different methods and bent under gravity loading. Though several attachment methods and cable designs were evaluated, only the selected configuration is presented in this paper.

The designed attachment method consists of Tapecoat H35 cold applied tape and 3M DP8010 structural plastic adhesive. The tape is applied longitudinally along the pipe over the sensing cable (Figure 3a). The tape provides initial adherence, holding the cable in place before the adhesive is applied. Next, the adhesive is injected under the tape at spacings of 1.5m (Figure 3b and 3c). The injected adhesive is then manually spread along the sensing cable by pressing on the injection site, forcing the epoxy to fill the void between the tape, cable and pipe surface along a length of approximately 30cm. Finally, the pipe was bent vertically using a forklift at the center (Figure 3d). The pipe was instrumented and then bent in the vertical plane.

Figure 3. Images from a bending test at UC Berkeley's Richmond Field Station. A) fully instrumented pipe before bending; B) epoxy injection process; C) final appearance after injection; D) forklift bending pipe by lifting at center

In this testing configuration, the springline of the pipe is the neutral axis (NA) of bending under elastic conditions. This location is expected to experience negligible bending strain. Any strain experienced by the NA is considered axial strain due to the pipe elongating during the vertical lift. Fiber optic sensing cables were placed at ±45° from the springline as well as at the crown. During elastic pure bending, the cables placed at the ±45° locations are expected to exhibit equal magnitude strain in compression and tension at the bottom and top of the pipe, respectively. These magnitudes are 70.7% $\left(\frac{\sqrt{2}}{2}\right)$ of the maximum bending strain, which would be experienced at the crown and invert of the pipe in this test case. Figure 4 shows this principle graphically. Since the bending stress is assumed to be linear elastic across the cross-section, so is the strain due to bending. The bending strain measured longitudinally at any location around the pipe circumference can be scaled by:

$$\varepsilon_{b,\max} = \frac{\varepsilon_{b,\beta}}{\sin(\beta)} \tag{1}$$

This produces the maximum bending strain experienced by the pipe. In the test case, this is expected at the pipe's top and bottom.

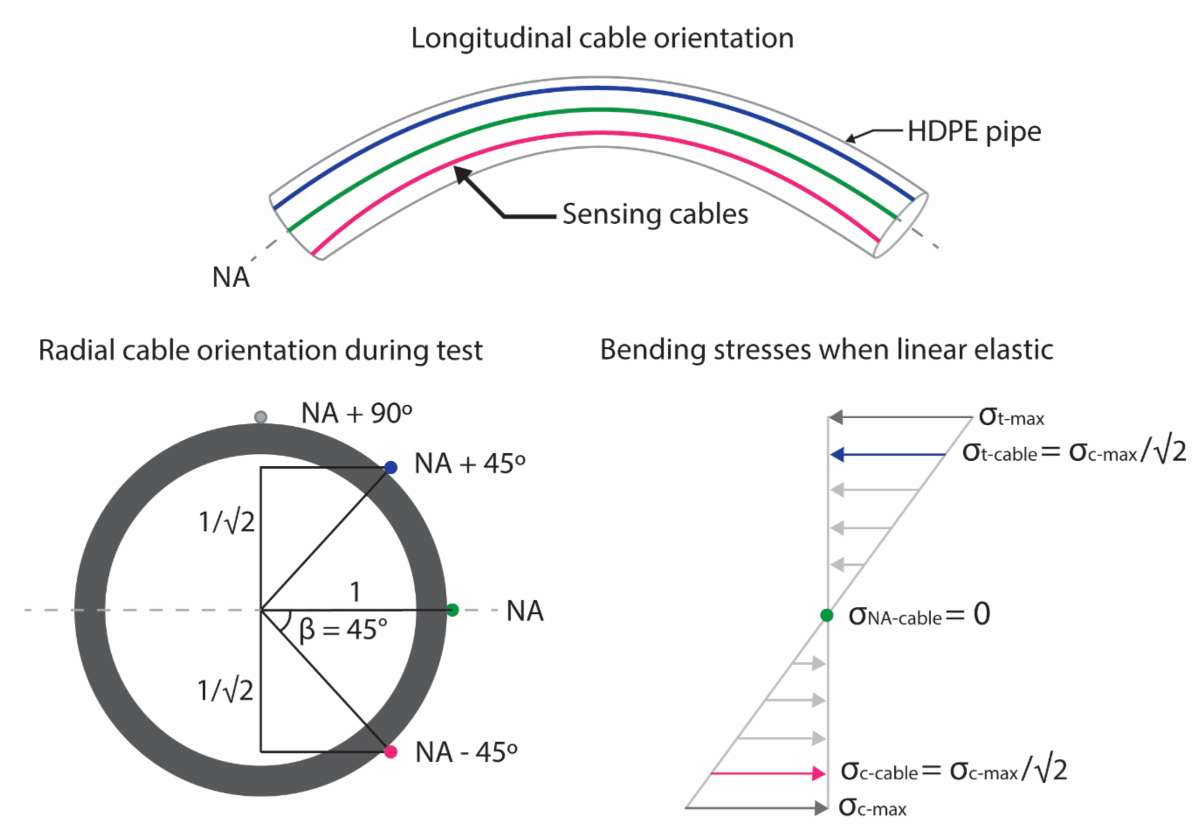

Figure 4. DFOS cable orientation and measurement magnitude during lab test

The strain measurements of the bending test are shown in Figure 5. The measurements show compressive strain at the sensing location toward the bottom of the pipe with a maximum magnitude of 750με (indicated as NA - 45°). The NA + 45° location experienced tensile strain with a maximum value of 1000με. The axial strain in the pipe, which can be viewed in this dataset as the strain at the neutral axis, acts as a positive shift in the measurements, which is why the compressive strain at the NA - 45° location is slightly less in magnitude than the tensile strain measurements at the NA + 45° location. The NA location (shown in green) experienced tensile strain with a maximum magnitude of 350 με. Slight tensile strain at the NA is expected due to the axial elongation experienced by the pipe during the vertical lift. This causes a maximum axial strain value towards the center of the pipe at the NA, which decreases towards the ends. Error in placement of the sensing cable at the NA or rotation of the pipe during bending are sources of error in this test. These profiles are next processed to calculate the pipe's deflection and compare with observations made during the test.

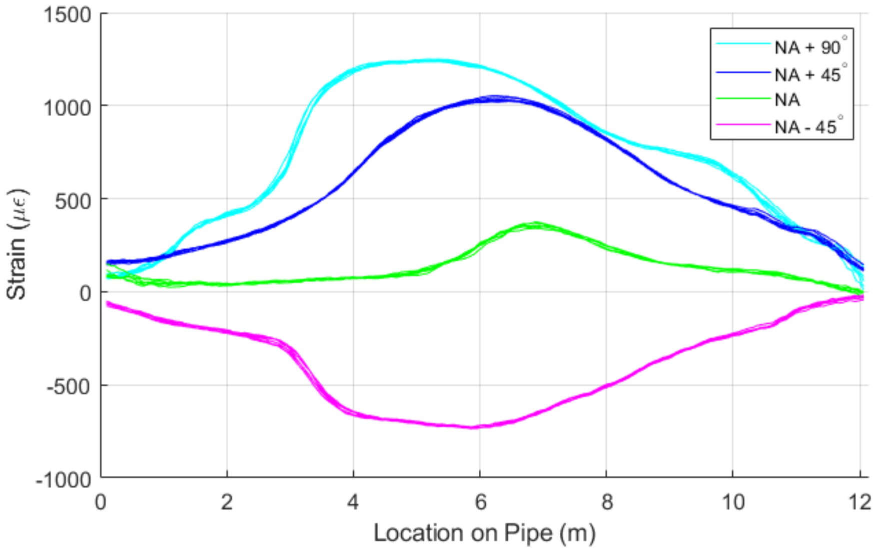

Figure 5. Distributed strain measurements made during the bending test

To determine the deformation of the pipe, the bending and axial strain must be calculated. This process is demonstrated using the NA, NA - 45° and NA + 45° cable locations. First, the axial strain, which is assumed uniform around the pipe circumference, is determined by taking the average of the three profiles. All calculations are conducted on vectors of data since there are measurements for every 2cm along the pipe. The following relationships are shown as continuous functions due to the brevity of notation.

$$\varepsilon_a(x) = \frac{1}{3}\left(\varepsilon_{NA}(x) + \varepsilon_{NA+45^\circ}(x) + \varepsilon_{NA-45^\circ}(x)\right) \qquad (2)$$

This value is then subtracted from the NA - 45° and NA + 45° profiles to calculate the strain that was only due to bending of the pipe.

$$\varepsilon_{b_{NA+45^\circ}}(x) = \varepsilon_{NA+45^\circ}(x) - \varepsilon_a(x) \qquad (3)$$

$$\varepsilon_{b_{NA-45^\circ}}(x) = \varepsilon_{NA-45^\circ}(x) - \varepsilon_a(x) \qquad (4)$$

Next, the maximum bending experienced by the pipe is calculated as the average of the absolute value of the profiles scaled by $\frac{1}{\sin(45^\circ)}$ due to the cable orientation.

$$\varepsilon_{b,max}(x) = \frac{\sqrt{2}}{2}\left(\left|\varepsilon_{b_{NA+45^\circ}}(x)\right| + \left|\varepsilon_{b_{NA-45^\circ}}(x)\right|\right) \qquad (5)$$

The resulting bending and axial strain profiles are shown in Figure 6.

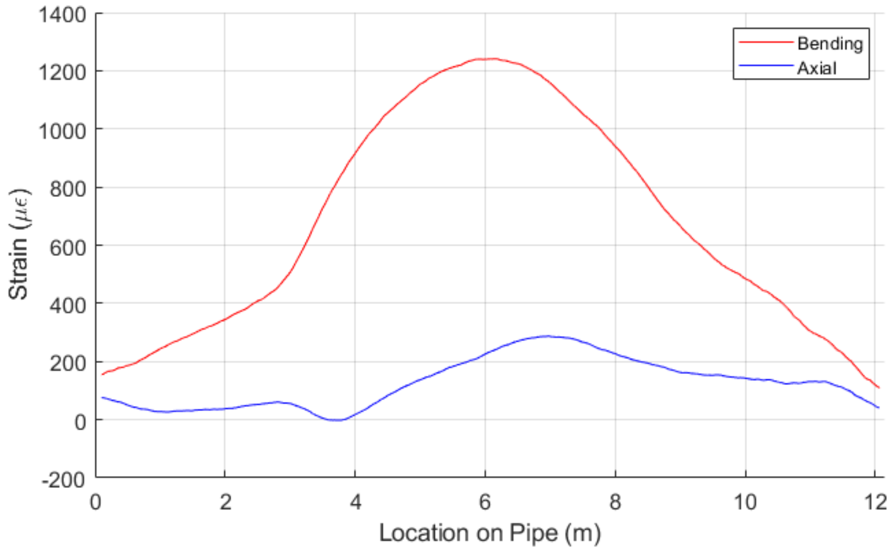

Figure 6. Axial and bending strain profiles during the bending test

The strain profiles can then be used to determine the deformation of the pipe due to axial and bending strain. Spatial integrations are conducted on the discrete data using the trapezoidal rule between adjacent readout channels. The vertical deflection due to bending strain is calculated by:

$$\kappa(x) = \frac{\varepsilon_{b-max}(x)}{c} \quad (6)$$

$$\theta(x) = \int_0^L \kappa(x)\, dx + C_1 \quad (7)$$

$$v_b(x) = \int_0^L \theta(x)\, dx + C_2 \quad (8)$$

It is crucial that the constants of integration be eliminated by boundary conditions. For this to occur, the instrumented section of pipe must have locations where the deflection and slope can be considered zero. In the test case, this occurs at the center of the pipe (L/2), so equations (7) and (8) can be rewritten as equations (9) and (10), respectively.

$$\theta(x) = \int_{\frac{L}{2}}^L \kappa(x)\, dx + \int_{\frac{L}{2}}^L \kappa(-x)\, dx \quad (9)$$

$$v_b(x) = \int_{\frac{L}{2}}^L \theta(x)\, dx + \int_{\frac{L}{2}}^L \theta(-x)\, dx \quad (10)$$

The deflection due to axial strain is then:

$$v_a(x) = \left[\int_{\frac{L}{2}}^L \varepsilon_a(x)\, dx + \int_{\frac{L}{2}}^L \varepsilon_a(-x)\, dx\right] \theta(x) \quad (11)$$

The total deflection is the sum of the contribution of bending and axial strain.

$$v_t(x) = v_a(x) + v_b(x) \qquad (12)$$

In the test case, the deflection due to axial strain was very low (<2mm). The total deflection profile as calculated from the DSTS measurements is shown in Figure 7. The deflection at the ends of the pipe is calculated from the measured data as 6.1 and 6.3cm. This agrees very well with measurements made with a tape measure at the ends of the pipe during bending, which were 6.5 and 6.8cm, respectively.

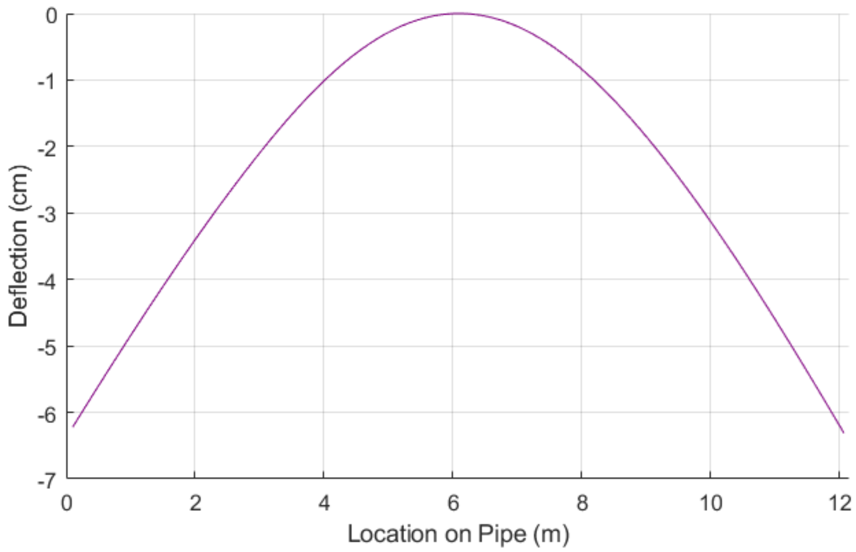

Figure 7. Deflection of the instrumented pipe during bending

FIELD INSTALLATION OF DSTS

Since the presented bending test was conducted over a very short amount of time, temperature compensation of the distributed strain measurements was not needed. In the field installation, strain will be measured over periods of time where temperature will fluctuate and impact the measurements. Therefore, a gel-filled strain-isolated cable will be installed adjacent to the pipe so that the impact of the temperature change on the strain measurements can be eliminated. Figure 8 shows the cable orientation that will be installed in the field. The orientation is a 90° rotation of the instrumentation demonstrated by the lab test, since the bending will be in the horizontal, rather than vertical, plane. The neutral axis of bending will be located at the crown of the pipe.

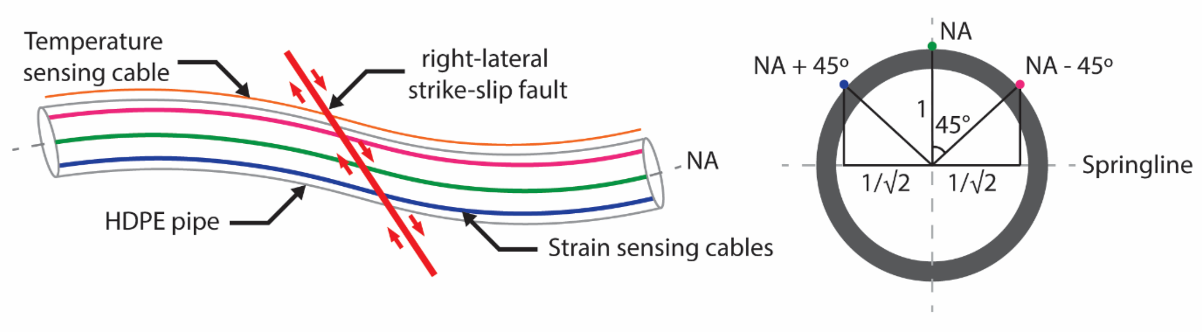

Figure 8. DSTS cable orientation and measurement magnitude during field installation

The pipe segments will be fused above ground and continuously pulled into the trench in as few segments as possible, as permitted by the allowable open trench length. When necessary, butt fusion will be performed in the trench to connect the segments after they are pulled into place. The sensing cables will be continuously attached to the pipe once it is placed within the trench. The sensing cables will extend at least 50m away from the fault zone on either side, so that sufficient zero-strain boundary conditions can be achieved. This is important so that the analysis method presented in equations (6)-(12) can be performed properly.

Additional considerations for the field installation include the backfill compaction method, backfill material gradation, construction staging and accommodation of fusion weld locations. Specifications and details for these considerations have been included into a full bid package and the awarded contractor will be responsible for developing a plan for construction staging and phasing.

CONCLUSIONS

A distributed sensing system to monitor the deformed shape of two HDPE pipelines crossing an active earthquake fault has been presented. Distributed strain and temperature sensing provides a solution to monitor critical pipelines when the deformation mechanism, magnitude and location is not well defined. A system that provides strain data every 2cm along a pipeline has been presented. The data can be processed to determine the axial and bending deformation experienced by the pipe through integration if there are known boundary conditions. This usually means instrumenting a length of pipe away from the expected deformation so a non-strained boundary can be defined in the data. An attachment method and cable type for the installation were also presented, completing a comprehensive distributed strain sensing system design for monitoring HDPE pipelines subject to ground deformation.

ACKNOWLEDGMENTS

The authors thank the staff of EBMUD’s Oakport facility and Llyr Griffiths of UC Berkeley’s Structures Laboratory for supporting the testing campaign.

REFERENCES

Lienkaemper, J. J., McFarland, F. S., Simpson, R. W., Bilham, R. G., Ponce, D. A., Boatwright, J. J., & Caskey, S. J. (2012). Long-term creep rates on the hayward fault: Evidence for controls on the size and frequency of large earthquakes. *Bulletin of the Seismological Society of America, 102*(1), 31-41. doi:10.1785/0120110033

Luo, L., Sekiya, H., & Soga, K. (2019). Dynamic distributed fiber optic strain sensing on movement detection. *IEEE Sensors Journal, 19*(14), 5639-5644. doi:10.1109/jsen.2019.2907889

O'Rourke, T., Jung, J., & Argyrou, C. (2016). Underground pipeline response to earthquake-induced ground deformation. *Soil Dynamics and Earthquake Engineering, 91*, 272-283. doi:10.1016/j.soildyn.2016.09.008

Kechavarzi, C., Soga, K., Battista, D. N., Pelecanos, L., B., E. M., & Mair, R. J. (2016). *Distributed fibre optic strain sensing for monitoring civil infrastructure: A practical guide*. London: ICE Publishing, a division of Thomas Telford.

Soga, K., Li, B., Yan, J., Luo, L., & Yu, Y. (2018). U.S. Patent No. WO2018005539A1. Washington, DC: U.S. Patent and Trademark Office

Soga, K., & Luo, L. (2018). Distributed fiber optics sensors for civil engineering infrastructure sensing. *Journal of Structural Integrity and Maintenance, 3*(1), 1-21. doi:10.1080/24705314.2018.1426138

Zhang, C., Shi, B., & Soga, K. (2019). Distributed Fiber Optic Sensing of Land Deformation: Methods and Case Studies. In *Selected papers from sessions of the Eighth International Conference on Case Histories in Geotechnical Engineering* (Vol. 311, pp. 188-196). Reston, VA: ASCE. doi:https://doi.org/10.1061/9780784482131